Flexible EMG arrays with integrated electronics for scalable electrode density

Philip M. Anschutz, Muneeb Zia, Jiaao Lu, Matthew J. Williams, Amanda L. Jacob, Samuel J. Sober, and Muhannad S. Bakir

345 Ferst Drive, Atlanta, GA, USA

E-mail: panschutz3@gatech.edu, mbakir@ece.gatech.edu

Abstract. Recent developments in electrode technology have demonstrated the power of flexible microelectrode arrays (FMEAs) for measuring muscle activity at high resolution. We recently introduced the Myomatrix array, a FMEA optimized for measuring the activity of individual motor units (the collection of muscle fibers innervated by a single motor neuron) [1] in freely behaving animals. Although FMEAs are fundamentally changing the way EMG is acquired, the number of recording channels is limited by the size of the plug that interfaces with the digital amplifier hardware and the density of electrode connections on the array. Increasing EMG channel count and supporting electrophysiological studies in smaller animals depends on two seemingly incompatible goals: reducing device size while increasing the number of recording channels. The solution to this is to increase channel density, which is currently limited by requiring that separate headstage and FMEA components be used simultaneously. In our prior devices [1], each FMEA had a dedicated wire output for every electrode input, creating a channel density is $1:1$. To improve this channel density, we have developed a novel device integrating a digital amplifier (bare-die RHD2216 chip, Intan, Inc. [6]) directly onto an FMEA. This new design reduces the device's backend footprint by 74% and relocates the intan bare die from the headstage to the FMEA itself, creating a channel density of $1:3.2$. Our methodology combines standard FMEA microfabrication with wire-bonding and surface-mounted components, enabling direct integration into a Serial Peripheral Interface (SPI) connection into the device itself, without any separate headstage. With this initial device we see a $1:3.2$ channel density, but our method allows for using other bare die amplifiers (Intan, Inc., USA) for a channel density of $1:12.8$. Our findings present a robust technique for chip embedding in custom FMEAs, applicable to in-vivo electrophysiology

1. Introduction:

1.1. The need for Application Specific EMG Devices

FMEA's have emerged as a new tool in measuring high signal-to-noise ratio (SNR) electromyography (EMG) applications. Being able to custom shape an electrode to a specific muscle target enables precise fit for the muscle, and places the electrodes in an

optimal location for recording. We recently introduced the Myomatrix array, a FMEA optimized for measuring the activity of individual motor units (the collection of motor units innervated by a single motor neuron [1]) in freely behaving animals.

While neural recording devices have advanced rapidly over the past decade, high resolution EMG devices have not seen the same advances in custom hardware that neural devices have experienced [15], [11]. While measuring neuron activity is one approach to behavioral neuroscience, measuring the output in EMG has its own advantages, and can provide another perspective. Combining these approaches can also be a powerful tool in diagnosing neuromuscluar disorders, like Parkinson's [10], ALS [7], and Alzheimer's disease [8]. Clinically there is a need for quantitative biomarkers for motor diseases. An example of this is the absence of a quantitative test for Parkinson's disease that can say if it is afflicting an individual [3]. With the Myomatrix arrays we have proven we can acquire high SNR EMG. There now exists a need to improve upon these devices to enable future studies in neuro-musclular disorders, and discover key biomarkers that could aid in disease discovery, and treatment [2].

1.2. Approaching Device Architecture

Recently there has been more interest in tailored applications for FMEA's that require smaller footprint devices, and increasing the number of electrodes that are present on the device [16] [12] [5]. While these seem like contradicting tasks, the advancements in the semiconductor industry have developed tools that can be applied to this problem. Currently we are not limited by electrode size requirements, meaning we can fabricate smaller electrodes on a smaller footprint FMEA. The limiting factor is the hardware requirements that would be needed to communicate with 10 times or 100 times the number of electrodes that are currently found in FMEA's. The solution to this is to increase channel density. In our prior devices [1], each FMEA had a dedicated wire output for every electrode input, creating a channel density is $1:1$. This is a fundamental design flaw that creates a bottleneck for increasing electrode count, and shrinking the device connections.

To create a device that is best suited for EMG applications the analog signal from the electrodes needs to be converted to a digital output on the device, and the device itself needs to be small enough to fit the animal model it is intended for. Another consideration is when scaling this device, we want to make it as user friendly as possible, and be able to plug into the RHD headstage amplifier board. For this reason, we have chosen to work with the INTAN RHD amplifier chip (INTAN INC, USA) . The specific chip chosen is the 2216, because it records from 32 bipolar (differential) channels which is well suited for long-term EMG recording. For the Myomatrix design we chose to work with a 32-channel array designed for a mouse forelimb recording from our previous work [1], due to the data we can compare our baseline to. Our approach is to build a robust implantation process that can be altered to the many different animal models that are used in EMG research. For our first device we chose a mouse model, and

created a render of the device to see if the size requirements of the embedded electronics themselves created a large advantage over the INTAN headstage. This render is shown in Figure 1. In this work, we propose a novel FMEA with an embedded INTAN 2216, to reduce the footprint of the device and increase channel density.

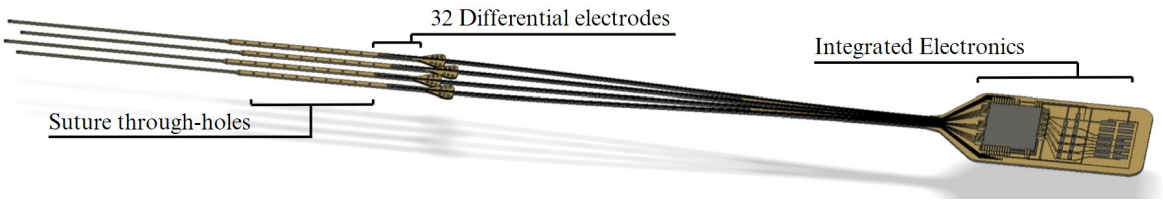

Figure 1. This render was used to see how small we could shrink the backend footprint of the device, and to see the size advantage it would have over the commercially available INTAN headstage

2. Methods

2.1. Design Resources

To begin we took the RHD 2216 headstage design and applied it to the backend of the 32-channel array designed for a mouse forelimb recording [1]. The design was constructed by taking the resources made available on INTAN's website [6], and recreating the connections on our device. The layout that we designed is shown in Figure 2.

2.2. Microfabrication

To begin, 15 µm of Polyimide (Pyralin 2611, HD Microsystems, USA) is spin coated onto a silicon handle wafer,and cured in a nitrogen environment. Adhesion Promoter (VM652, HD Microsystems, USA) is applied to the outer edge of the wafer to prevent peeling during the process. After curing, a metal liftoff forms the traces for the device. We use an electron beam evaporator to deposit 20 nm Ti and then 300 nm Au. After a 12 hour liftoff, VM652 is spin coated on the entire wafer, and then the top Polyimide is spin coated to 3 µm. After curing, positive resist is patterned to make an etch mask. A reactive ion etch (Vision RIE, $O_2 : SF_6$ with a $5 : 1$ ratio) opens the electrodes and the connections for the surface mount components and the wirebonding pads. Next we thicken the wirebonding pads so that they are compatible with commercial wirebonders. To achieve this another liftoff process with 300nm Cu and 20nm Au is deposited on the open pads on the backend of the device as seen in 3.

2.3. Benchtop Assembly

After removing the device from the cleanroom it is moved to a benchtop workspace to mount the surface mount components (SMC). To mount these a stencil was made to "screen print" conductive epoxy on the surface of the Flex array. For the stencil we

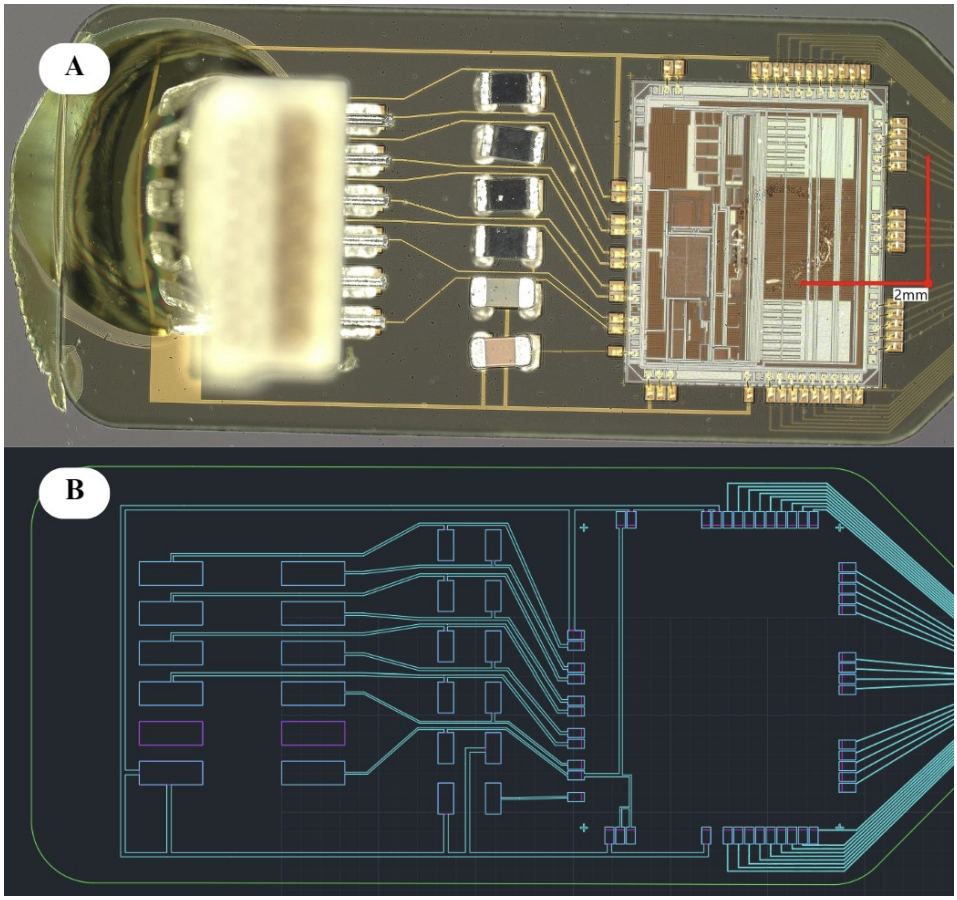

Figure 2. Routing Diagram for Embedded INTAN 2216. (A) is the finished device with, an omnetics connection, resistors, capacitors, and the RHD2216 chip wirebonded to the flex array. (B) depicts the routing of the device, and highlights the routing of the analog connections under the chip itself.

used a 500 µm thick blue spring steel that was laser diced using an Optec Femtosecond laser. The conductive epoxy was applied by using a glass slide to press the epoxy through the spring steel and the 4 resistors (0402, Taiyo Yuden, JPN) , 2 capacitors (0402, Panasonic, JPN), and omnetics connector(A79623, Omnetics Corp, USA) were placed by hand under a microscope. After this testing of the flex array from the top of the omnetics connector to all points of SMC's was conducted to make sure device is functioning properly before chip placement. We measured approximately 20 Ω trace impedance from the connector to the surface mount components, and this ensured that the device was assembled correctly. Next, the INTAN RHD 2216 is placed using a vacuum pencil and secured using devcon epoxy. Wirebonding using 25um gold wire was then used to integrate the chip. After wirebonding the device is tested by plugging the device into the recording hardware and ensuring the device is recognized by the software. Next the device is covered in Devcon epoxy to ensure that the device is biocompatible (the copper and conductive epoxy need to be insulated), and that the device has rigidity to be removed from the handle wafer. After the epoxy is cured the polyimide array is

laser diced using the Optec Femtosecond laser which creates the shape of the device, and removed from the handle wafer.

2.4. Impedance Testing

After the device was finished, we tested the performance by measuring the impedance. For this we plugged in the device through the SPI cable to an INTAN RHD aquisition board in slot A. Next approximately 8 ml of sterile saline solution (0.9% NaCl, AddiPak, USA) was deposited on the electrodes of the device while the device was still on the handle wafer. A ground wire was attached to the aquisition board, and the other end was submerged in the saline solution approximately 5mm from the electrodes. At this time we ran the impedance test 3 times on the 16 bipolar electrodes. This is a function of the INTAN open access interface that works with the acquisition board and can be aquired from INTAN's website [6].

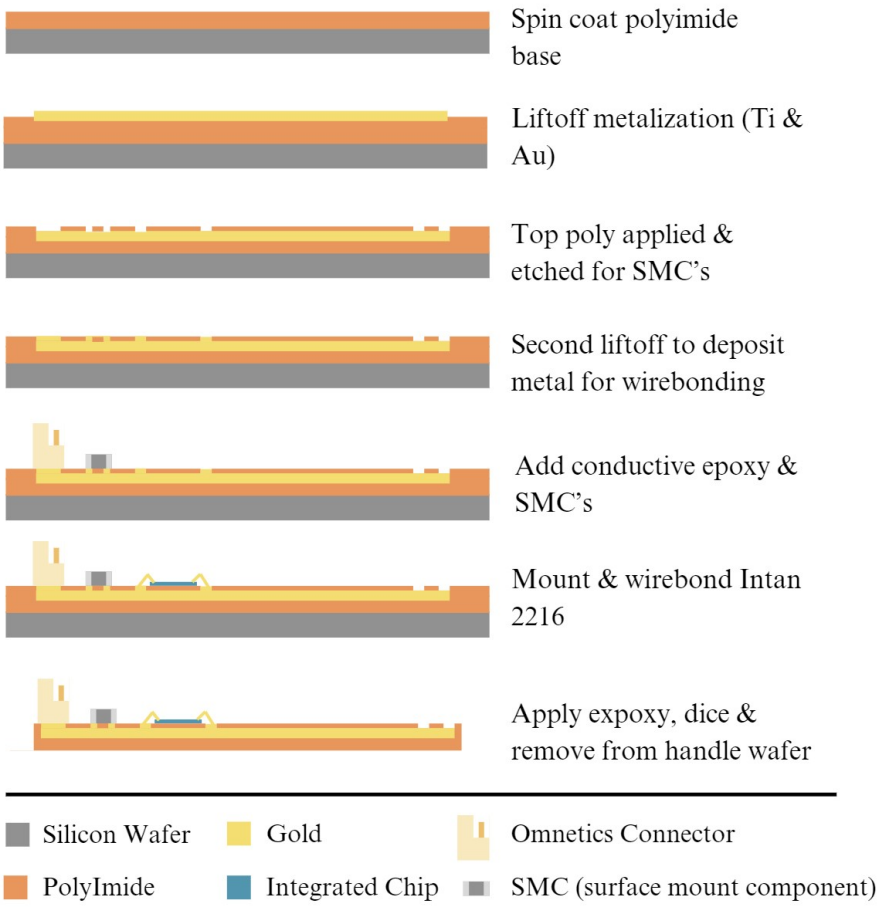

Figure 3. An overview of the process including microfabrication, and benchtop assembly

2.5. Device Implantation

All procedures were approved by the Emory University Institutional Animal Care and Use Committee. An adult C57BL/6 mouse was anesthetized within an anesthesia chamber using 2 %(vol/vol) isoflurane in oxygen gas before being placed supine while continuing to provide an anesthesia plane. After confirming the proper depth of anesthesia, the digastric muscle was revealed through an incision made under the jaw, and the fascia surrounding the digastric muscle was removed. The digastric muscles were chosen to test the electrode array due to ease of access and its high rate of spontaneous EMG activity while under anesthesia. The electrode array was placed on the muscle surface, and spontaneous single-unit EMG was collected through an RHD 512-channel recording controller (Part number C3004; Intan Technologies) recording at 30 Hz using a computer running RHX Data Acquisition Software (Intan Technologies.)

3. Results

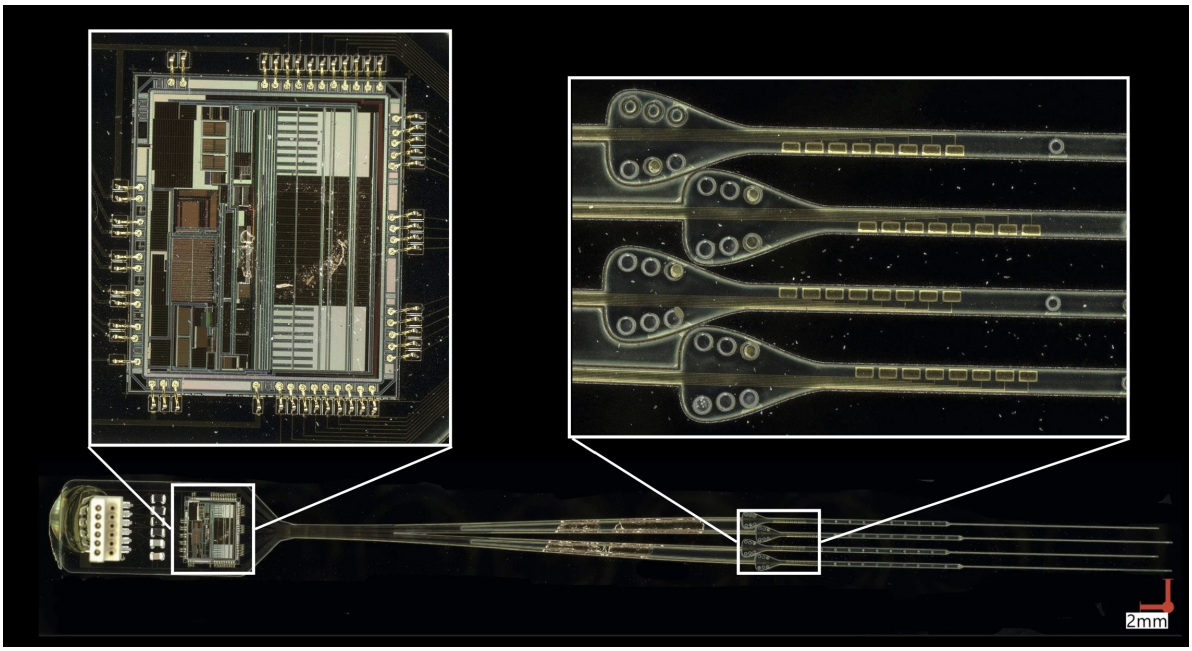

Figure 4. A darkfield microscope image highlights two features of the device, the 51 wirebonds that connect the bare die to the flex array, and secondly the electrodes which have the dimensions of 100 µm by 200 µm. These electrodes are in a series of 8 linear electrodes per thread, which was designed for mouse forelimb recording. The tabs on the electrodes, as well as the vias assist with handling the electrodes, and attaching them to a muscle.

Multiple devices were fabricated to test the reliability of this method, and the features of this design supported our goal of reducing the footprint by 74% and increasing the channel density from 1 : 1 to 1 : 3.2. The electrodes, and the 51 wirebonds are shown in Figure 4. For the footprint we measured twice, first with digital calipers,

and second with a confocal microscope. Both methods measured the same reduction in footprint size, with the caliper measurements shown in Figure 7.

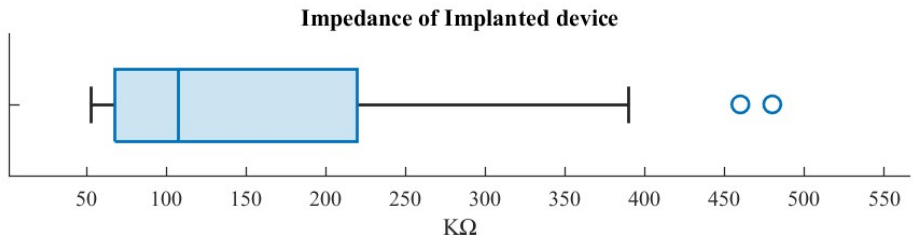

Figure 5. The impedance was measured three times at 1KHz, and each of the 16 bipolar channels recorded a discrete entry.

Testing the electric characteristics of the device to ensure performance was similar to current FMEA's was measured ensure that the recording quality was not affected by the device architecture. The impedance measurements show that the device performed as expected, with impedances measuring between 60 KΩ, and 600 KΩ, with a distribution of all electrode impedances shown in Figure 5. These impedances are similar to other gold pad electrodes, and can be improved by adding PEDOT:PSS [9]. Other recent studies show that this level of impedance is acceptable for spike sorting applications [4]. Comparing this device's baseline impedance to previous impedance baselines in the Myomatrix workshop, confirms we are within the threshold for single motor unit detection, as depicted in Figure 6.

After electrical characterization, the device was implanted *in-vivo* in an acute setting, on a mouse's digastric muscle [9]. We chose the digastric muscle due to the amplitude of the spike, and that it is active while the mouse is sedated. We were able to gather data over a 20 minute period that was comparable to measuring with the previous FMEA + INTAN Heastage demonstrated in the Myomatrix arrays. In Figure 6, we show sections of the recordings that have the identifiable motor unit waveform.

4. Discussion

4.1. Channel density

By demonstrating a robust method to integrate bare die chips onto FMEA's we can see that we are already successful in creating a higher channel density. This device has a channel density of 1 : 3.2, which is achieved through the 2216 bare die. The method does not apply to just this chip, with INTAN's bare die offerings we can combine RHS (stimulation chips) and higher electrode count RHD (recording chips) bare die to create higher channel density, and control different experiment types. Without changing the method and applying the design changes to the substrate, we can combine multiple RHD2164 bare die to increase channel density even further. For smaller animals we must consider the target muscle ensuring the device does not become too bulky, while increasing channel density. The advantage of this, for EMG specifically, lies in the

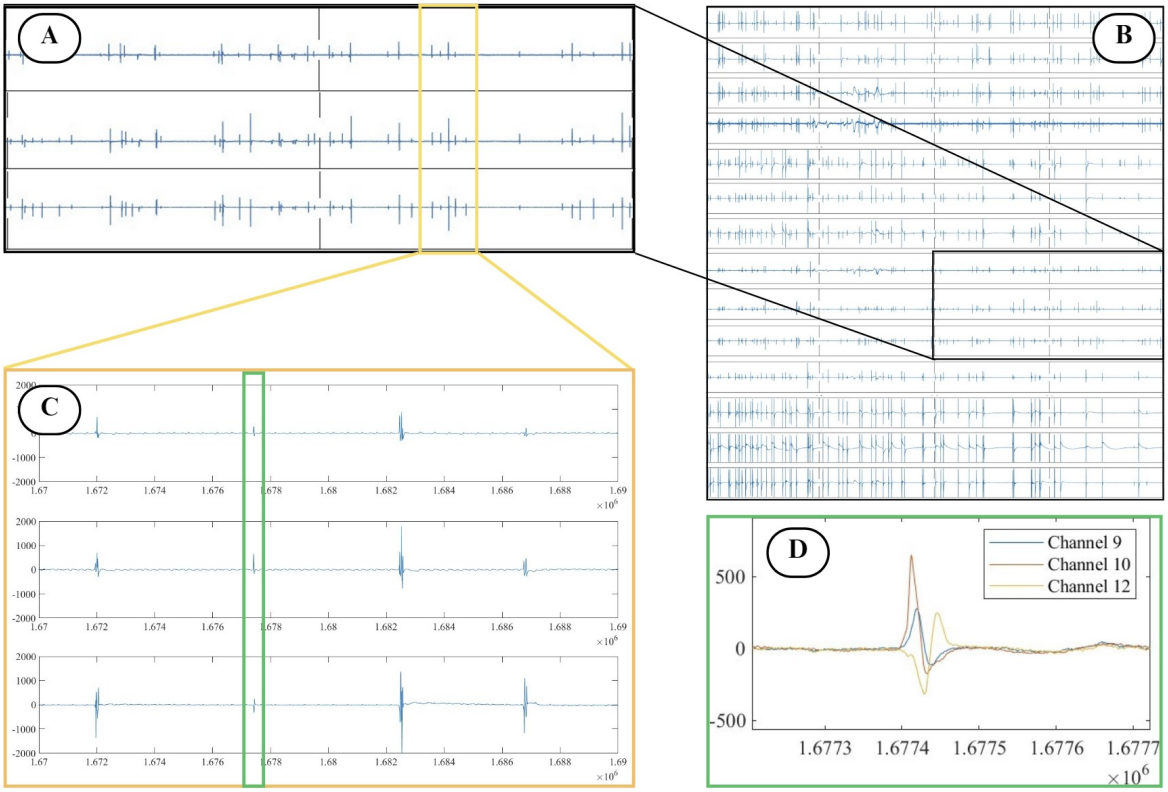

Figure 6. (A) This is a subset of channels with an exceptionally low noise floor, that are all on the same thread as seen in Figure 4. (B) An overview of all channels (C) Higher resolution subset of the channels shown in A, with timing in ms, and the amplitude set to ± 2000 mV. (D) is an overlay of C showing the change in amplitude across channels 9, 10, and 12 for the same motor unit

flexible substrate that can be cut to match any muscle structure, and the size of the electrodes can be designed accordingly to fit the muscle. With the high SNR capabilities of these devices, these improvements will create a higher quality data set.

4.2. Advantages for natural behavior studies

Comparing the size of the device in Figure 7, shows how much of an advantage this device has when compared to the previous FMEA. These measurements in Figure 7 (A) were aquired with calibrated calipers, and then again with a microscope to ensure that the 74% footprint reduction was accurate. The new device can be implanted subcutaneously with only an SPI connection mounted on the animal's periphery, enabling new studies that require a smaller footprint. The previous FMEA's Omnetics connector is 3 times larger, and would inhibit long term studies that could take advantage of this smaller device. If you consider the size advantages in integrating bare die vs packaged chips you can save space and weight. A recent study [14] showcases a rat headstage that uses 4 packaged chips for data aquisition, and using this wirebonding method they would be able to get rid of the plastic packaging, saving space and weight on the headstage.

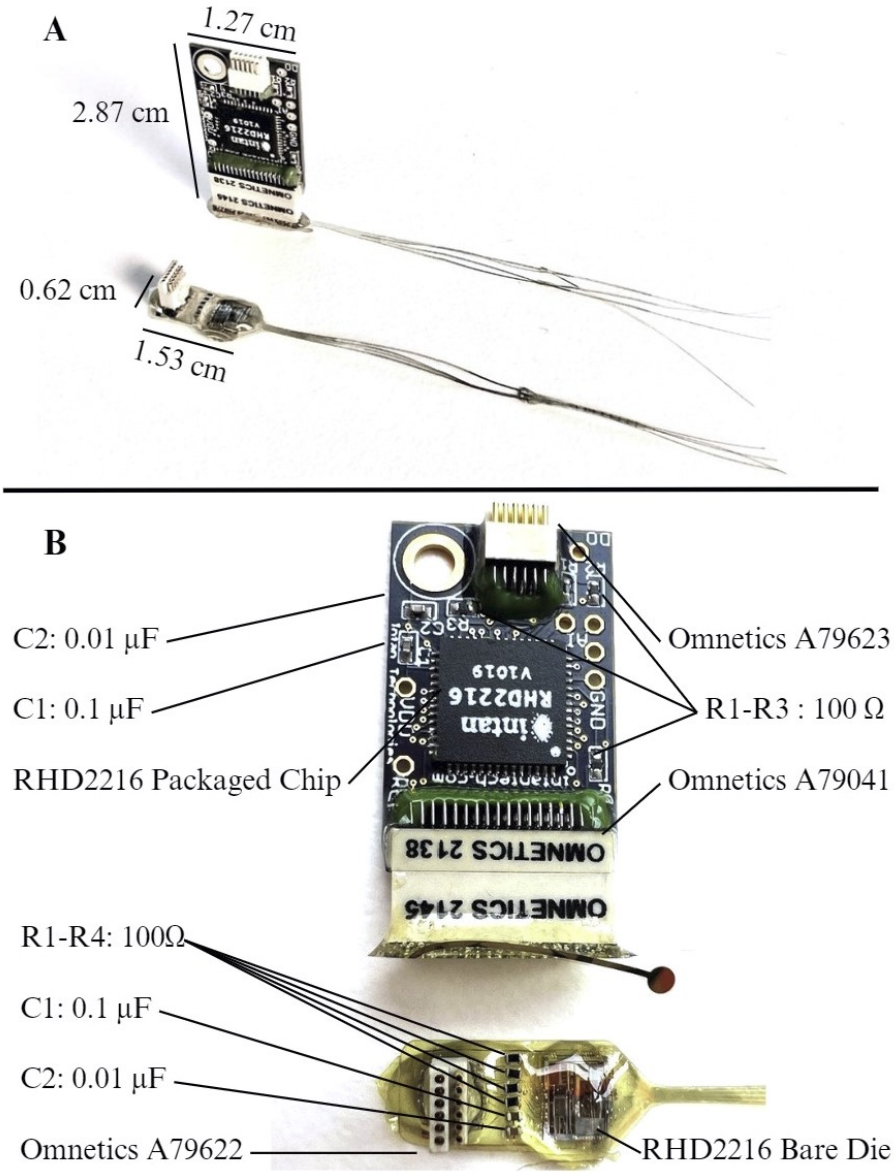

Figure 7. (A) Comparison of the size of the commercially available INTAN headstage to the embedded device. (B) The layout of the INTAN headstage vs the layout of the flex array. Note the use of space on the flex array is much more compact.

Another consideration in freely behaving animal studies, you want to minimize the changes to the animal's physiology as much as possible to retain natural behavior. With this wirebonding approach it not only improves upon this goal, but also will be less of a burden for the animal to carry around, improving the animals quality of life. For larger animals like primates, this may not pose a large advantage, but for mice the added weight of the large connector affects its head weight and angular momentum. Early studies in freely behaving mice with headstages used many methods to circumvent this issue including attaching helium balloons to the headstage to reduce the load on the

animal [13]. This weight and angular momentum of a headstage will affect the animal's movement and therefore alter it's EMG data. Aside from the data, creating a device that is more comfortable for the animal will improve its quality of life during the study, and is ethically responsible.

4.3. Conclusion

With the Myomatrix's introduction we demonstrated a device that can acquire high resolution EMG capable of detecting single motor units. This enabled a new quantitative data set that can be used to study neuromuscular disorders, like Parkinsons, and ALS. With this novel device we have addressed a critical design flaw that created a bottleneck when increasing the number of electrodes. This new device architecture we can continue to increase the electrode count, and keep a small, bio-compatible device footprint. To conclude, this research presents a robust process to reduce the footprint of the device and increase channel density, while being applicable to all types of *in-vivo* electrophysiology.

5. Acknowledgement

We would like to thank the faculty and staff of the Institute for Electronics and Nanotechnology for their effort in supporting this work, especially Mr. Chris White who helped optimize the wire-bonding process. Many thanks also to Dr. Visvesh S. Sathe, Professor of Electrical Engineering at Georgia Institute of Technology and Dr. Reid Harrison of INTAN Inc. for helpful suggestions when troubleshooting the embedded INTAN bare die.This work was supported by The McKnight Foundation, The Simons Foundation, and grants: NIH R01NS084844, NIH R01NS099375, NIH R01EB022872, NSF 1822677, NIH R01NS109237, U24NS126936.

6. Ethical Statement

All animal procedures were approved by the Emory University Institutional Animal Care and Use Committee.

References

[1] Bryce Chung et al. "Myomatrix arrays for high-definition muscle recording". en. In: *eLife* 12 (Nov. 2023). DOI: 10.7554/eLife.88551.2. URL: https://elifesciences.org/reviewed-preprints/88551 (visited on 04/23/2024).

[2] Stuart F. Cogan. "Neural stimulation and recording electrodes". eng. In: *Annual Review of Biomedical Engineering* 10 (2008), pp. 275–309. ISSN: 1523-9829. DOI: 10.1146/annurev.bioeng.10.061807.160518.

[3] George DeMaagd and Ashok Philip. "Parkinson's Disease and Its Management". In: *Pharmacy and Therapeutics* 40.8 (Aug. 2015), pp. 504–532. ISSN: 1052-1372. URL: https://www.ncbi.nlm.nih.gov/pmc/articles/PMC4517533/ (visited on 06/06/2024).

[4] Juyeon Han et al. "Impact of Impedance Levels on Recording Quality in Flexible Neural Probes". en. In: *Sensors* 24.7 (Jan. 2024), p. 2300. ISSN: 1424-8220. DOI: 10.3390/s24072300. URL: https://www.mdpi.com/1424-8220/24/7/2300 (visited on 04/23/2024).

[5] Bruce Harland et al. "A Subdural Bioelectronic Implant to Record Electrical Activity from the Spinal Cord in Freely Moving Rats". en. In: *Advanced Science* 9.20 (July 2022), p. 2105913. ISSN: 2198-3844, 2198-3844. DOI: 10.1002/advs.202105913. URL: https://onlinelibrary.wiley.com/doi/10.1002/advs.202105913 (visited on 06/27/2024).

[6] *Intan Technologies*. en-US. URL: https://www.intantech.com (visited on 06/20/2024).

[7] Nanette C Joyce and Gregory T Carter. "Electrodiagnosis in Amyotrophic Lateral Sclerosis". In: *PM & R : the journal of injury, function, and rehabilitation* 5.5 0 (May 2013), S89–S95. ISSN: 1934-1482. DOI: 10.1016/j.pmrj.2013.03.020. URL: https://www.ncbi.nlm.nih.gov/pmc/articles/PMC4590769/ (visited on 06/11/2024).

[8] Lampros C. Kourtis et al. "Digital biomarkers for Alzheimer's disease: the mobile/wearable devices opportunity". en. In: *npj Digital Medicine* 2.1 (Feb. 2019), pp. 1–9. ISSN: 2398-6352. DOI: 10.1038/s41746-019-0084-2. URL: https://www.nature.com/articles/s41746-019-0084-2 (visited on 06/06/2024).

[9] Jiaao Lu et al. *High-performance Flexible Microelectrode Array with PEDOT:PSS Coated 3D Micro-cones for Electromyographic Recording*. en. Feb. 2022. DOI: 10.1101/2022.02.03.479004. URL: https://www.biorxiv.org/content/10.1101/2022.02.03.479004v1 (visited on 04/23/2024).

[10] Alexander Y. Meigal et al. "Non-Linear EMG Parameters for Differential and Early Diagnostics of Parkinson's Disease". In: *Frontiers in Neurology* 4 (Sept. 2013), p. 135. ISSN: 1664-2295. DOI: 10.3389/fneur.2013.00135. URL: https://www.ncbi.nlm.nih.gov/pmc/articles/PMC3775312/ (visited on 06/06/2024).

[11] Elon Musk. "An Integrated Brain-Machine Interface Platform With Thousands of Channels". In: *Journal of Medical Internet Research* 21.10 (Oct. 2019), e16194. ISSN: 1439-4456. DOI: 10.2196/16194. URL: https://www.ncbi.nlm.nih.gov/pmc/articles/PMC6914248/ (visited on 04/23/2024).

[12] Tao Sun et al. *High-Stability Polyimide-based Flexible Electrodes with IrO $_x$ to Interface the Mouse Vagus Nerve*. en. May 2021. DOI: 10.1101/2021.05.10.442867. URL: http://biorxiv.org/lookup/doi/10.1101/2021.05.10.442867 (visited on 06/27/2024).

[13] Kun Xie et al. "512-Channel and 13-Region Simultaneous Recordings Coupled with Optogenetic Manipulation in Freely Behaving Mice". English. In: *Frontiers in Systems Neuroscience* 10 (June 2016). ISSN: 1662-5137. DOI: 10.3389/fnsys.2016.00048. URL: https://www.frontiersin.org/articles/10.3389/fnsys.2016.00048 (visited on 06/20/2024).

[14] Tansel Baran Yasar et al. "Months-long tracking of neuronal ensembles spanning multiple brain areas with Ultra-Flexible Tentacle Electrodes". en. In: *Nature Communications* 15.1 (June 2024), p. 4822. ISSN: 2041-1723. DOI: 10.1038/s41467-024-49226-9. URL: https://www.nature.com/articles/s41467-024-49226-9 (visited on 06/20/2024).

[15] Zhiwen Ye et al. "Ultra-high density electrodes improve detection, yield, and cell type identification in neuronal recordings". eng. In: *bioRxiv: The Preprint Server for Biology* (Apr. 2024), p. 2023.08.23.554527. DOI: 10.1101/2023.08.23.554527.

[16] Mengjia Zhu et al. "Flexible Electrodes for In Vivo and In Vitro Electrophysiological Signal Recording". en. In: *Advanced Healthcare Materials* 10.17 (Sept. 2021), p. 2100646. ISSN: 2192-2640, 2192-2659. DOI: 10.1002/adhm.202100646. URL: https://onlinelibrary.wiley.com/doi/10.1002/adhm.202100646 (visited on 06/27/2024).